The following publication C. Wang et al., "Bragg Gratings in Suspended-Core Photonic Microcells for High-Temperature Applications," in Journal of Lightwave Technology, vol. 36, no. 14, pp. 2920-2924, 15 July, 2018 is available at https://doi.org/10.1109/JLT.2018.2831258.

Bragg Gratings in Suspended-Core Photonic Microcells for High-Temperature Applications

Chao Wang, Jingchuan Zhang, Congzhe Zhang, Jun He, Yuechuan Lin, Wei Jin, *Senior Member, IEEE*, Changrui Liao, Ying Wang, and Yiping Wang, *Senior Member, IEEE*

***Abstract*—We report a novel type-II photonic crystal fiber Bragg grating for high-temperature applications. The Bragg grating is inscribed in a low-loss in-fiber structure named suspended-core photonic microcell, which is postprocessed from a commercial pure-silica photonic crystal fiber. Grating samples with core diameters of about 4 μm were made by using a focused near-infrared femtosecond laser and a phase mask, and then tested in a tube furnace from room temperature to about 1200 °C. The thermal response of the Bragg resonant wavelength was measure to be about 12 and 16 pm/°C, respectively, at the temperature around 100 °C and 1000 °C. The grating spectrum remained stable in a 10-h isothermal annealing at 1000 °C and started decaying at about 1120 °C with the rate of about 0.02 dB/min. This type of grating possesses flexibilities in both waveguide and grating structure design, exhibits good high-temperature performance, hence would be promising platform for building wavelength-division-multiplexed fiber sensors and tunable devices with a wide working temperature range.**

***Index Terms*—High-temperature techniques, optical fiber devices, optical fiber measurements, photonic crystal fiber Bragg grating.**

I. Introduction

OPTICAL fiber Bragg gratings (FBGs) are widely used devices in various applications, especially for the scenarios requiring multi-point measurements and sustainability in harsh environments, for example, with intense electromagnetic interference, high radiation, cryogenic or high temperature *et al.* [1] For the ordinary ultraviolet (UV)-laser-induced type-I gratings in standard single mode fibers (SMFs), the upper limit of operation temperature is ∼500 °C [2]. The high-temperature performance of FBG can be largely improved by making type-II grating using lasers with high peak-power and short-duration pulse, such as femtosecond (fs) laser or nanosecond UV excimer laser. Such gratings are typically formed by local structural changes induced by a threshold dependent multiphoton ionization process, and would withstand temperature up to ∼1000 °C [3]. The type-II grating inscribed in Sapphire crystal fiber can even be applied at 1900 °C for temperature sensing [4]. However, the sapphire fibers are difficult to be spliced to commercial silica fibers, and highly multimode with wide grating peaks. In addition, the regeneration of a type-I grating would form a new grating which can survive at temperature up to 1295 °C [5], but the fabrication of such grating might be time consuming in the processes of hydrogen loading and thermal treatment [6].

The Bragg grating inscription techniques have been applied on the fibers with micro-structures for seeking enhanced grating properties and extended functions, which may be introduced by the flexible in-fiber structures [7]–[9]. The gratings inscribed in pure-silica photonic crystal fibers (PCFs) have been reported by using excimer laser [10] and fs lasers [11], [12]. Since these gratings would decay at the temperature of ∼500 °C [10], [11], they might be type-I gratings. The scattering and distortion of the side incident inscription laser in the periodic cladding structures are the major factors hampering the formation of a type-II gratings in PCFs [13]. A relief FBG was fabricated in PCF by using a laser etching technique. With the aid of a thin toluene layer preloaded on the capillary wall of PCF, periodic scratches would be formed on the capillary walls after exposing to the grating inscription laser. This grating demonstrated good thermal stability up to ∼940 °C [14]. In the micro-structured fiber with simple cladding, such as the suspended-core fiber (SCF), side incident beam can reach the fiber core with little cladding disturbance. Type-II Bragg grating inscribed in SCF can survive at temperature up to 1300 °C [15], but the connection loss between SCFs and the widely used standard SMF system might be a problem in practical applications.

Here we report a novel high temperature Bragg grating made in a locally processed PCF by using a focused fs laser and a phase mask. The simple cladding geometry of the processed PCF

This work was supported in part by the National Natural Sci-ence Foundation of China under Grants 61405125 and 61290313; in part by the CAST Innovation Foundation under Grant CAST-BISEE2017-015; in part by the Science and Technology Innovation Commission of Shenzhen under Grant JCYJ20150324141711614; and in part by the China Postdoctoral Science Foun-dation under Grants 2015M572351 and 2016T90796. *(Corresponding author: Yiping Wang.)*

C. Wang is with the Key Laboratory of Optoelectronic Devices and Systems of Ministry of Education and Guangdong Province, College of Optoelectronic Engineering, Shenzhen University, Shenzhen 518060, China, and also with the School of Electrical Engineering, Wuhan University, Wuhan 430072, China (e-mail: eecwang@whu.edu.cn).

J. Zhang is with the Beijing Institute of Spacecraft Environment Engineering, Beijing 100094, China (e-mail: jcw1014@163.com).

C. Zhang, Y. Lin, and W. Jin are with the Department of Electrical Engineering, Hong Kong Polytechnic University, Hong Kong (e-mail: congzhe. zhang@polyu.edu.hk; lin.yuechuan@connect.polyu.hk; eewjin@polyu.edu. hk).

J. He, C. Liao, Ying Wang, and Yiping Wang are with the Key Laboratory of Optoelectronic Devices and Systems of Ministry of Education and Guang-dong Province, College of Optoelectronic Engineering, Shenzhen University, Shenzhen 518060, China (e-mail: hejun07@szu.edu.cn; cliao@szu.edu.cn; yingwang@szu.edu.cn; ypwang@szu.edu.cn).

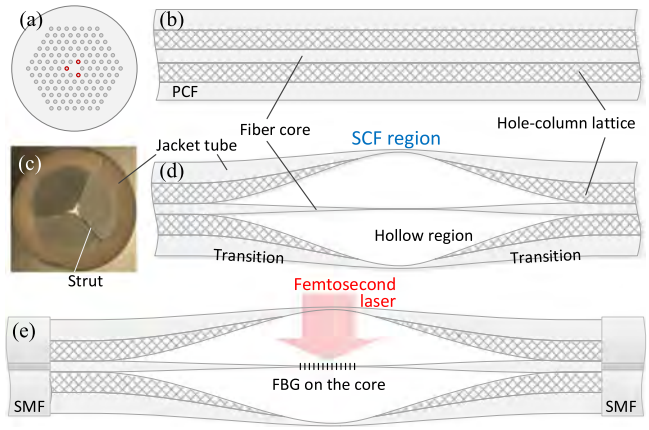

Fig. 1. Schematics of a commercial PCF (ESM-12) from (a) axial and (b) transverse directions. (c) The cross-sectional micrograph of a three-hole suspended-core fiber (SCF) region which was made by selectively inflating the red-marked columns in (a). (d) Typical structure of a suspended-core photonic microcell. (e) Bragg grating inscription at the selectively inflated region.

region allows the direct lateral inscribing of type-II grating in the fiber core. Comparing to the other common high temperature FBGs [1], [16], this grating possesses extra features of the holey in-fiber region isolated from environmental contamination, and the micro-/nano-sized core with strong evanescent-field, which would be useful for light-matter interaction applications.

II. Fabrication of the Grating

The pure-silica PCF (model ESM-12) from NKT photonics Co. was used in fabricating the gratings for high temperature applications. The typical transvers and axial cross-sectional structures of the PCF are illustrated in Fig. 1(a) and (b). In this fiber, light would propagate along the central defect of the hole-column lattice (photonic crystal) region. Before grating inscription, the PCF was firstly selectively pressurized through the three red-marked hole-columns in Fig. 1(a), and then heated to the softening temperature of silica at a target position. In few minutes, a section of three-hole SCF with typical structure as Fig. 1(c) would form in the heated region under the coaction of gas pressure and surface tension of softened silica. Fig. 1(b) and (d) are, respectively, the schematics of a PCF before and after the selectively inflation process. Obviously, pressurizing different air-columns in Fig. 1(a) would produce SC-PMC with different internal structures. The fabrication details of the local SCF region, i.e., suspended-core photonic microcell (SC-PMC), was reported in [17], [18]. Comparing to the SCFs directly drawn from the fiber tower, the SC-PMC can be spliced into SMF network with optimized loss below 0.2 dB by virtue of the similar mode pattern between ESM-12 PCF and standard SMF.

During the inflation process in the SC-PMC fabrication, most of the cladding hole-columns of the PCF would collapse. Hence, as shown in Fig. 1(e), laser beams can be focused onto the fiber core from fiber side with little scattering and distortion, which would facilitate the formation of high quality gratings in the fiber core. Several first-order Bragg gratings have been realized in the SC-PMCs with different core sizes by use of a Ti:sapphire fs laser (800 nm, 100 fs, 1 kHz), a phase mask with pitch of

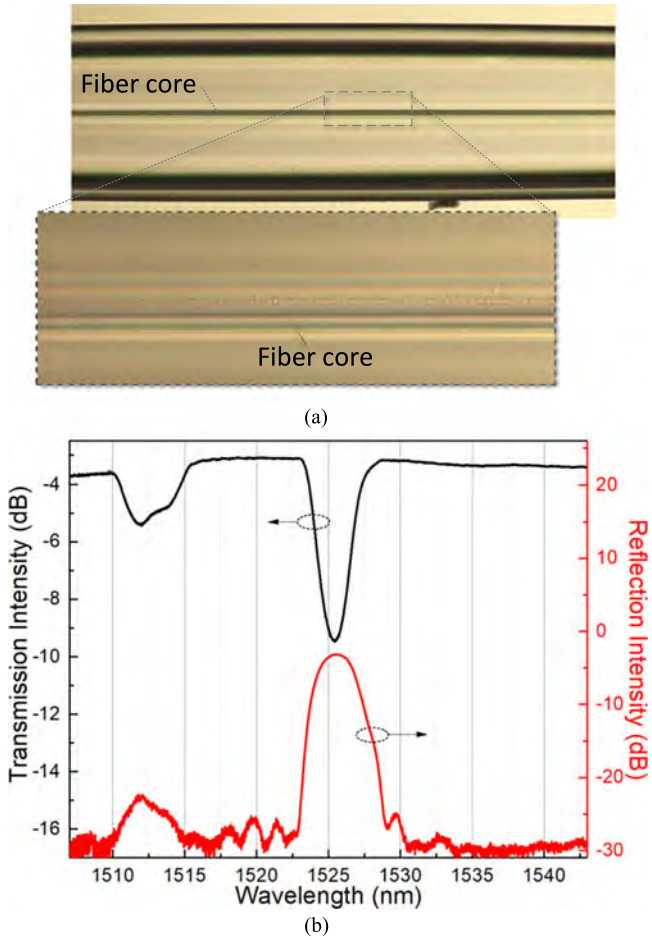

Fig. 2. (a) Micrographs of a SC-PMC grating sample from side direction. Inset: zoom in image of fiber core in the grating region. (b) Transmission and reflection spectra of a SC-PMC grating sample with core diameter of $\sim$4 μm.

1070 nm and a cylindrical lens with focal length of 50 mm. A CCD cameras was used in the fabrication to guarantee the good alignment between the laser focus and fiber core [19].

The upper image of Fig. 2(a) shows a sample of the Bragg grating embedded SC-PMC with outer diameter of $\sim$200 μm and core diameter of $\sim$4 μm. The grating sample was fabricated by using fs laser pulse energy of $\sim$260 μJ and exposure time of 18 minutes. Near the processed core region, scratches on struts of the SC-PMC can be observed [see the lower image in Fig. 2(a)]. The periodic scratches would induce structural modulations to the fiber core, resulting in the formation of a type-II grating.

As a proof-of-concept demonstration, here we report the investigation on high temperature endurance and decaying process of the gratings in the SC-PMC. The grating samples under test possessed the cross-sectional structure as Fig. 1(c) and core diameter of $\sim$4 μm. The transmission and reflection spectra of such a grating sample are given in Fig. 2(b). The sample has a Bragg dip intensity of $\sim$6.4 dB in transmission spectrum and a side-mode suppression ratio of $\sim$22 dB in reflection. The wide 3-dB bandwidth of $\sim$2 nm could be explained by the chirp effects induced by the tapered shape of the fiber core or/and the Gaussian shape of the fs laser beam. The bandwidth could be

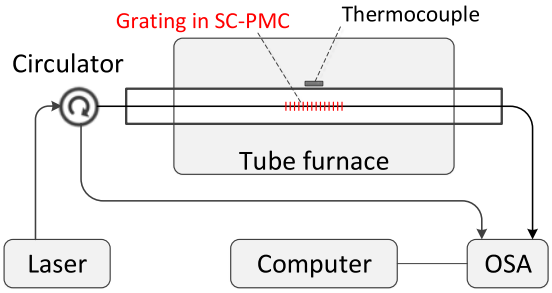

Fig. 3. Experimental setup for testing high temperature performance of the gratings inscribed in SC-PMCs.

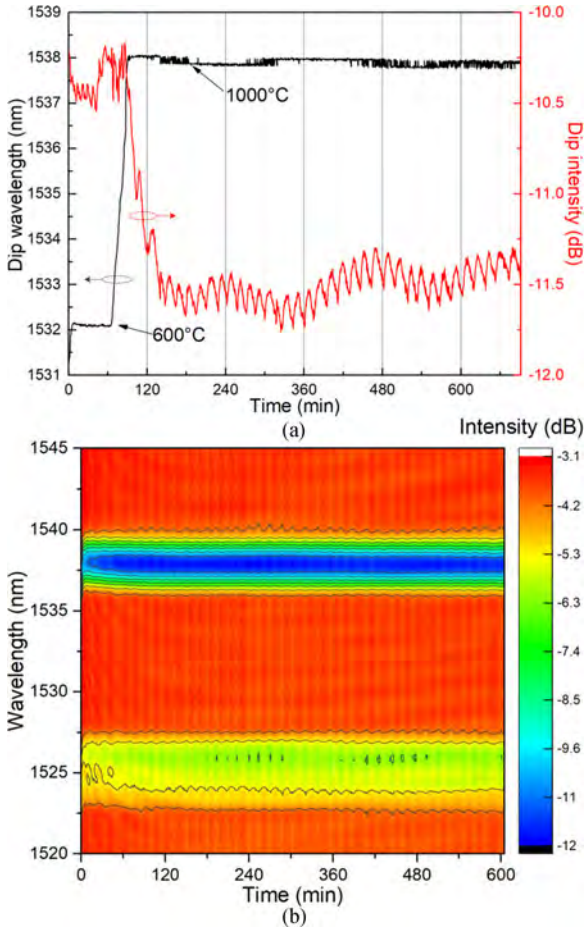

Fig. 4. (a) The dip wavelength and intensity as functions of time in two isothermal annealing in consequence. (b) The spectral evolution of the grating sample at 1000 °C. The upper ribbon is the Bragg resonant dip in transmission and the lower ribbon is the higher order mode resonant dip.

narrowed by using SC-PMC with longer uniform region or/and extending the grating length with an updated inscription system. Loss of the sample is ∼3.4 dB, however, it can be optimized to less than 0.5 dB in the SC-PMC with smaller core size [19].

III. High-Temperature Characterization

The grating samples were tested in a tube furnace (Carbolite GERO MTF12-38-250) to investigate their temperature response, thermal durability and degradation characteristics. Fig. 3 is the setup of the test system. The samples were placed in the

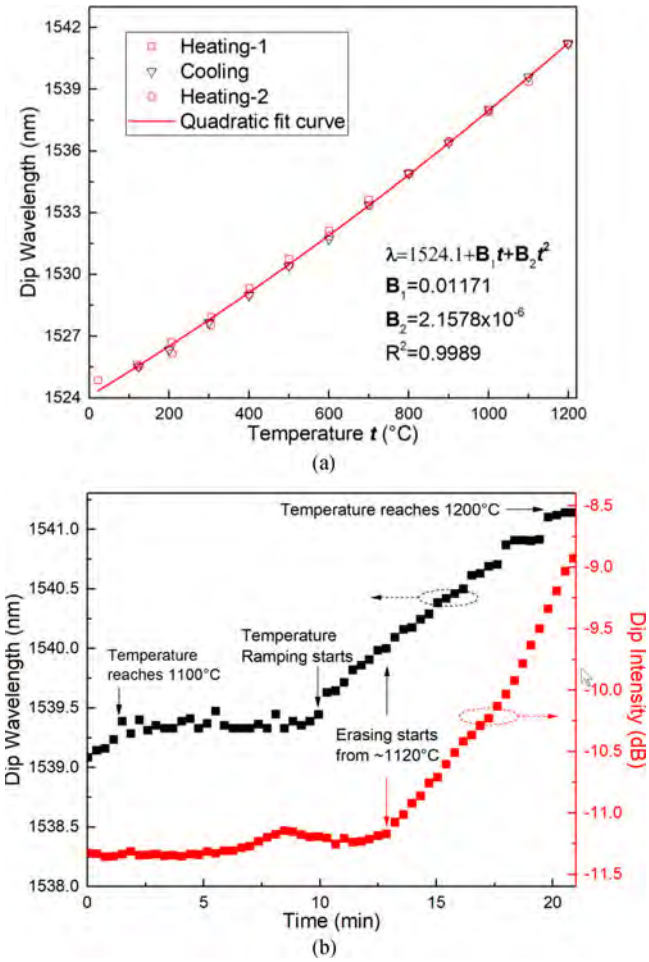

Fig. 5. (a) The response of grating wavelength to the temperature in a range from 22 °C to 1200 °C. (b) Dip wavelength and intensity of grating as functions of time in an isochronal annealing from 1100 °C to 1200 °C.

central uniform region (±5 °C, 90-mm-length) of the furnace, in which the temperature was PID controlled by using wire wound heater and monitored with an embedded N-type thermocouple. The transmission and reflection spectra of the samples were measured by using a wideband laser source (Amonics ALS-CWDM-FA), an optical fiber circulator and an optical spectrum analyzer (OSA, Yokogawa AQ6319).

The sample in Fig. 2 was isothermally annealed firstly at 600 °C for 1 hour and then at 1000 °C for 10 hours. During the process, evolution of grating spectra was measured every 25 seconds. The curves in Fig. 4(a) are the grating wavelength and intensity as functions of the annealing time in the process. Fig. 4(b) is the evolution of dips of Bragg resonant and higher order mode resonant dips at 1000 °C. The grating dip wavelength was stable in both of the annealing processes at 600 °C and 1000 °C. The dip intensity experienced a growth of ∼1.1 dB in the first 50 minutes after the temperature reaching 1000 °C, meanwhile, the loss also increased ∼0.3 dB. A similar grating intensity strengthening was also observed in the high temperature annealing process of the relief gratings inscribed on the capillary walls of PCFs [14]. This phenomenon could be explained by the thermal decomposition of the small residue of

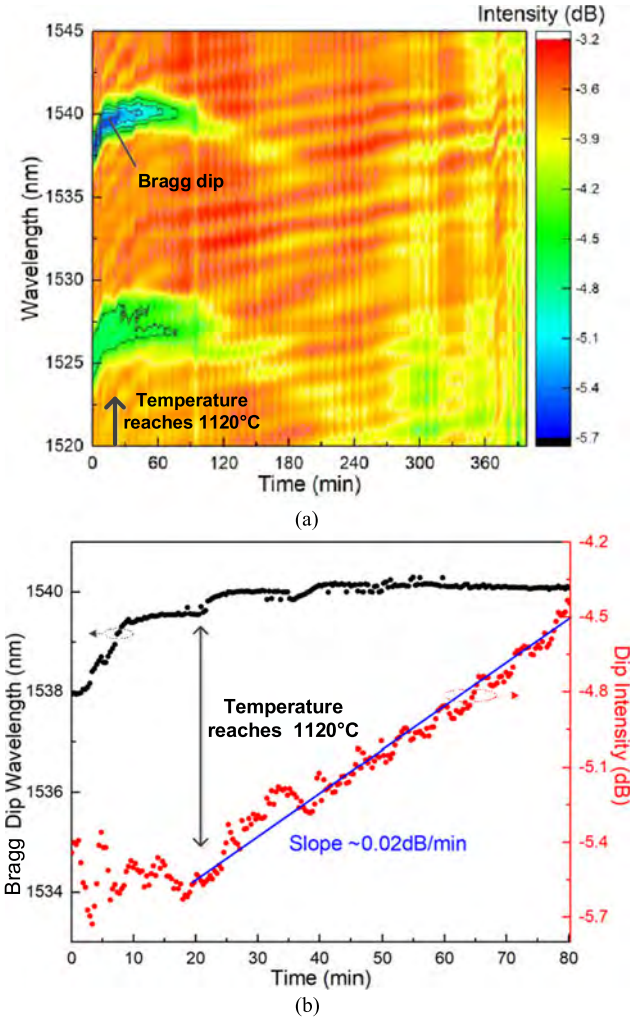

Fig. 6. (a) The spectral evolution of a second grating sample in a 6.5-hour isothermal annealing test at 1120 °C. (b) The changes of Bragg dip wavelength and intensity of the sample as functions of the time in the decaying process.

debris covering the grating. The oscillation with amplitude of ∼0.2 dB in the grating intensity in Fig. 4(a) and the spectra ripple in Fig. 4(b) should be induced by the heating cycles of the furnace which has a period of ∼18 min. The tests results demonstrate a stable fs-laser-ablation grating in SC-PMC at elevated temperatures till 1000 °C.

In the next experiment, the thermal response of the annealed grating was then tested from room temperature (∼22 °C) to 1200 °C with the step of 100 °C. Fig. 5(a) shows the Bragg resonant wavelength of the sample as functions of temperature in two heating and one cooling processes. The sample's Bragg wavelength demonstrated a nonlinear thermal response which can be fit with a quadratic curve: $\lambda = 1524.1 + B_1 t + B_2 t^2$ ($B_1 = 0.01171, B_2 = 2.1578 \times 10^{-6}$). The sensitivity was ∼12 pm/°C at the temperature around 100 °C, and increased to ∼16 pm/°C at ∼1000 °C, which was believed to be mainly determined by the temperature-induced refractive-index (RI) change of the fiber material [20]. It worth to note that the fitting curve would be only valid for the grating samples with particular parameters such as the core diameter, cross-sectional geometry, the holey region RI and the grating structure.

When the furnace temperature isochronally ramped from 1100 °C to 1200 °C with rate of 5 °C/min, the decaying of grating dips was observed. As shown in Fig. 5(b), the sample was firstly heated to 1100 °C and stayed there for ∼10 min. In this period of time, the dip intensity remains stable without obvious decaying. In the followed heating process, the erasing effect of the grating dips started from ∼1120 °C which might indicate the highest operating temperature of such gratings. The decaying rate increased to about 0.5 dB/min when temperature is close to 1200 °C.

Another grating sample with the same core size and grating period, i.e., the same Bragg wavelength, was tested to study the isothermal decaying process of the grating at 1120 °C, where the erasing effect started. Compare to the last sample, this grating has a weaker intensity of ∼5.7 dB and a similar loss of ∼3.5 dB. Fig. 6(a) shows the evolution of grating spectrum in a 6.5-hour isothermal test, in which most of the grating dips disappeared in ∼1 hour. In the followed 5-hour test, the loss of the erased sample increased ∼0.5 dB and no regeneration of grating happened. Fig. 6(b) shows the Bragg wavelength and intensity as functions of time in the decaying process. The intensity decaying rate of the grating is estimated to be ∼0.02 dB/min at 1120 °C.

IV. Conclusion and Discussion

High temperature performance of the fs-laser-ablation Bragg gratings built in a pure-silica SC-PMC have been comprehensively investigated. Samples of the grating can withstand high temperature up to ∼1100 °C. The temperature response of a grating sample with core diameter of ∼4 μm at optical communication wavelength was ∼12 pm/°C at the temperature around 100 °C, and increased to ∼16 pm/°C at ∼1000 °C, which could be explained by the variance of thermal-optics coefficient of fiber material at different temperatures. Bragg resonant of the sample exhibited good long-term stability at 1000 °C and started to decay at ∼1120 °C with the rate of ∼0.02 dB/min.

This type of grating offers a flexible platform for building wavelength-division-multiplexed sensors and tunable devices with wide working temperature range. Gratings with different properties could be engineered by building various grating s in PMCs with different structure parameters. For example, Bragg gratings made in SC-PMC with highly birefringent [21] would exhibit two Bragg resonant dips, which would be applied in dual parameter sensing; Parallel gratings could be inscribed in the multi-core SC-PMC by the point-by-point inscription technique and used as a bending vector sensor. In addition, various materials can be filled in the protected evanescent-filed region of the grating. This would enable further extension of the grating's application fields.

References

[1] S. J. Mihailov, "Fiber Bragg grating sensors for harsh environments," *Sensors*, vol. 12, no. 2, pp. 1898–1918, 2012.

[2] T. Erdogan, V. Mizrahi, P. J. Lemaire, and D. Monroe, "Decay of ultraviolet-induced fiber Bragg gratings," *J. Appl. Phys.*, vol. 76, no. 1, pp. 73–80, 1994.

[3] D. Grobnic, C. W. Smelser, S. J. Mihailov, and R. B. Walker, "Long-term thermal stability tests at 1000 °C of silica fibre Bragg gratings made with ultrafast laser radiation," *Meas. Sci. Technol.*, vol. 17, no. 5, pp. 1009–1013, 2006.

[4] T. Habisreuther, T. Elsmann, Z. Pan, A. Graf, R. Willsch, and M. A. Schmidt, "Sapphire fiber Bragg gratings for high temperature and dynamic temperature diagnostics," *Appl. Thermal Eng.*, vol. 91, pp. 860–865, 2015.

[5] J. Canning, M. Stevenson, S. Bandyopadhyay, and K. Cook, "Extreme silica optical fibre gratings," *Sensors*, vol. 8, no. 10, pp. 6448–6452, 2008.

[6] J. Canning, "Regeneration, regenerated gratings and composite glass properties: The implications for high temperature micro and nano milling and optical sensing," *Measurement*, vol. 79, pp. 236–249, 2016.

[7] C. M. Jewart, Q. Wang, J. Canning, D. Grobnic, S. J. Mihailov, and K. P. Chen, "Ultrafast femtosecond-laser-induced fiber Bragg gratings in air-hole microstructured fibers for high-temperature pressure sensing," *Opt. Lett.*, vol. 35, no. 9, pp. 1443–1445, 2010.

[8] A. P. Zhang *et al.*, "Microfluidic refractive-index sensors based on small-hole microstructured optical fiber Bragg gratings," *Appl. Phys. Lett.*, vol. 98, no. 22, 2011, Art. no. 221109.

[9] A. Cusano, D. Paladino, and A. Iadicicco, "Microstructured fiber Bragg gratings," *J. Lightw. Technol.*, vol. 27, no. 11, pp. 1663–1697, Jun. 2009.

[10] N. Groothoff, J. Canning, E. Buckley, K. Lyttikainen, and J. Zagari, "Bragg gratings in air-silica structured fibers," *Opt. Lett.*, vol. 28, no. 4, pp. 233–235, 2003.

[11] L. Fu *et al.*, "Femtosecond laser writing Bragg gratings in pure silica photonic crystal fibres," *Electron. Lett.*, vol. 41, no. 11, pp. 638–640, 2005.

[12] A. Saliminia, A. Proulx, and R. Vallée, "Inscription of strong Bragg gratings in pure silica photonic crystal fibers using UV femtosecond laser pulses," *Opt. Commun.*, vol. 333, pp. 133–138, 2014.

[13] F. Berghmans, T. Geernaert, T. Baghdasaryan, and H. Thienpont, "Challenges in the fabrication of fibre Bragg gratings in silica and polymer microstructured optical fibres," *Laser Photon. Rev.*, vol. 8, no. 1, pp. 27–52, 2014.

[14] M. Konstantaki, P. Childs, M. Sozzi, and S. Pissadakis, "Relief Bragg reflectors inscribed on the capillary walls of solid-core photonic crystal fibers," *Laser Photon. Rev.*, vol. 7, no. 3, pp. 439–443, 2013.

[15] S. C. Warren-Smith, L. V. Nguyen, C. Lang, H. Ebendorff-Heidepriem, and T. M. Monro, "Temperature sensing up to 1300 °C using suspended-core microstructured optical fibers," *Opt. Express*, vol. 24, no. 4, pp. 3714–3719, 2016.

[16] C. Liao and D. Wang, "Review of femtosecond laser fabricated fiber Bragg gratings for high temperature sensing," *Photon. Sens.*, vol. 3, no. 2, pp. 97–101, 2012.

[17] C. Wang, W. Jin, W. Jin, J. Ju, J. Ma, and H. L. Ho, "Evanescent-field photonic microcells and their applications in sensing," *Measurement*, vol. 79, pp. 172–181, 2016.

[18] C. Wang, W. Jin, J. Ma, Y. Wang, H. L. Ho, and X. Shi, "Suspended core photonic microcells for sensing and device applications," *Opt. Lett.*, vol. 38, no. 11, pp. 1881–1883, 2013.

[19] C. Wang *et al.*, "Bragg gratings inscribed in selectively inflated photonic crystal fibers," *Opt. Express*, vol. 25, no. 23, pp. 28442–28450, 2017.

[20] A. D. Kersey *et al.*, "Fiber grating sensors," *J. Lightw. Technol.*, vol. 15, no. 8, pp. 1442–1463, Aug. 1997.

[21] C. Wang *et al.*, "Highly birefringent suspended-core photonic microcells for refractive-index sensing," *Appl. Phys. Lett.*, vol. 105, no. 6, 2014, Art. no. 061105.